Palmprint Verification with Moments

Ying-Han Pang[1] Andrew T.B.J[1] David N.C.L[1] Hiew Fu San[2]

[1]Faculty of Information Science and Technology
Multimedia University
Jalan Ayer Keroh Lama
75450, Melaka, Malaysia.

[2]Faculty of Engineering and Technology
Multimedia University
Jalan Ayer Keroh Lama
75450, Melaka, Malaysia.

yhpang@mmu.edu.my bjteoh@mmu.edu.my david.ngo@mmu.edu.my fshiew@mmu.edu.my

ABSTRACT

Palmprint verification is an approach for verifying a palmprint input by matching the input to the claimed identity template stored in a database. If the dissimilarity measure between the input and the claimed template is below the predefined threshold value, the palmprint input is verified possessing same identity as the claimed identity template. This paper introduces an experimental evaluation of the effectiveness of utilizing three well known orthogonal moments, namely Zernike moments, pseudo Zernike moments and Legendre moments, in the application of palmprint verification. Moments are the most commonly used technique in character feature extraction. The idea of implementing orthogonal moments as palmprint feature extractors is prompted by the fact that principal features of both character and palmprint are based on line structure. These orthogonal moments are able to define statistical and geometrical features containing line structure information about palmprint. An experimental study about verification rate of the palmprint authentication system using these three orthogonal moments as feature descriptors has been discussed here. Experimental results show that the performance of the system is dependent on the moment order as well as the type of moments. The orthogonal property of these moments is able to characterize independent features of the palmprint image and thus have minimum information redundancy in a moment set. Pseudo Zernike moments of order of 15 has the best performance among all the moments. Its verification rate is 95.75%, which also represents the overall performance of this palmprint verification system.

Keywords

Verification, Image Features, Zernike Moments, Pseudo Zernike Moments, Legendre Moments, Orthogonality.

1. INTRODUCTION

Palmprint authentication is one of the relatively new physiological biometric technologies which exploit the unique features on the human palmprint, namely principle lines, wrinkles, ridges, datum points, etc as shown in Figure 1. The rich texture information of palmprint offers the effective means in person authentication due to its non-intrusive, user friendly, stable, low-resolution imaging and low cost requirements [Shu98a][You02a]. This has drawn considerable interest and attention to researchers especially from academia.

Journal of WSCG, Vol.12, No.1-3, ISSN 1213-6972
WSCG'2004, February 2-6, 2003, Plzen, Czech Republic.

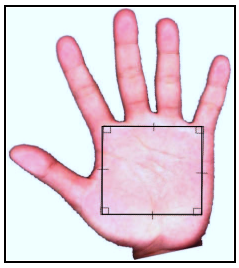

Figure 1. Palmprint.

An important issue in palmprint recognition is to extract palmprint features that can discriminate an individual from the other. There are two popular approaches to palmprint recognition. One of the approaches is to transform palmprint images into specific transformation domains. Among the works that appear in the literature are eigenpalm [Lu03a],

Gabor filters [Wai03a], Fourier Transform [Li02a], and wavelets [Kum02a]. Another approach is to extract principal lines and creases from the palm [Dav99a][Dut02a][Wu02a][You02a]. However, this method is not easy because it is sometimes difficult to extract the line structures that can discriminate every individual well. Besides, creases and ridges of the palm are always crossing and overlapping each other, which complicates the feature extraction task. Chinese character is similar to palmprint, which is also constructed from the line structures, and moments have been utilized for shape extraction for long time [Wu02a]. Moment can describe Chinese character uniquely regardless how close the characters are in terms of local features. This inspired us to implement the moments function to extract the palmprint ridges and creases for the human verification tasks.

In this paper, we had implemented Zernike moments (ZM), pseudo Zernike moments (PZM) and Legendre moments (LM) as feature descriptors in the application of human palmprint verification. These approaches are able to provide adequate information about different types of statistical and geometrical information of the creases and ridges in the palmprint image. Orthogonal basis of the moments can attain a zero value of redundancy measure in a set of moment functions, so that these orthogonal moments correspond to independent characteristics of the image [Muk98a]. In other words, minimum information redundancy in a moment set is obtained. Moments' geometrical invariance promote themselves as commonly used feature extraction approaches in a broad spectrum of applications in image analysis, such as invariant pattern recognition, reconstruction, object classification and etc. [Muk98a].

Our palmprint verification is generally composed of four stages. In the first stage, localization of palmprint region is implemented. Furthermore, the localized palmprint image (region of interest) is enhanced by means of local histogram equalization. The second stage involves feature extraction by using ZM, PZM and LM as feature descriptors. Determination of pertinent and optimal order moments in feature extraction is performed in this stage, too. Euclidean distance is applied to compute the dissimilarity measure of the palmprint for the purpose of feature matching in the third stage. The final stage requires decision making whether a claimant should be accepted or rejected.

This paper is organized under six sections. Section 2 presents palmprint image preprocessing and feature extraction algorithms: Zernike moments (ZM), pseudo Zernike moments (PZM) and Legendre moment (LM), are introduced in section 3. Section 4 describes palmprint verification based on orthogonal moments' features. Section 5 shows the experimental results and discussion about the experimental result is having in this section, too. Conclusion is discussed in section 6.

2. PALMPRINT PREPROCESSING

In the palmprint acquisition stage, users are allowed to place their palms freely on the platform of the scanner when scanning is performed. Therefore, palmprint images captured in the image acquisition stage may have variable size and orientation and also subject to noise. Moreover, the region of not-interest (e.g fingers, wrist, image background, etc) may affect accurate processing and degrade the verification performance. Therefore, image preprocessing is a crucial and necessary part before feature extraction.

In this study, the region of interest (ROI) is extracted from the palmprint images. The ROI in this paper is defined in a square shape after the correction of orientation. Then the ROI is converted to a fixed size (150 x 150 pixels) so that all of the palmprints conform to a same size. The details of preprocessing can be referred in [Tee02a]. The localized palmprint is depicted in Figure 2.

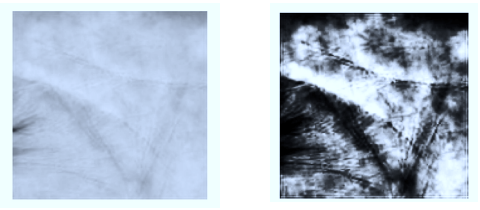

(a) (b)

Figure 2. The localized palmprint (a) Palmprint before enhancement (b) Palmprint after enhancement.

3. FEATURE EXTRACTION

Feature extraction is defined as a process of converting a captured biometric sample, i.e palmprint, into a unique, distinctive and compact form so that it can be compared to a reference template. According to [Hu62a], moment sequence, M_{pq} is uniquely determined by the image $f(x,y)$ and conversely, $f(x,y)$ is uniquely described by $M_{pq.}$ The uniqueness of the moment method prompted us to its suitability in palmprint feature extraction. Furthermore, orthogonality property of the ZM, PZM and LM enables redundancy reduction among their respective description and thus help to improve the computation efficiency.

3.1. Zernike Moments

The kernel of Zernike moments is a set of orthogonal Zernike polynomials defined over the polar coordinate space inside a unit circle. The two-dimensional Zernike moments of order p with repetition q of an image intensity function $f(r,\theta)$ are defined as:

$$Z_{pq} = \frac{p+1}{\pi} \int_0^{2\pi} \int_0^1 V_{pq}(r,\theta) f(r,\theta) r dr d\theta \; ; |r| \le 1 \qquad (1)$$

where Zernike polynomials $V_{pq}(r,\theta)$ are defined as:

$$V_{pq}(r,\theta) = R_{pq}(r) e^{-\hat{j}q\theta} \; ; \quad \hat{j} = \sqrt{-1} \qquad (2)$$

and the real-valued radial polynomials, $R_{pq}(r)$, is defined as follows:

$$R_{pq}(r) = \sum_{k=0}^{\frac{p-|q|}{2}} (-1)^k \frac{(p-k)!}{k!\left(\frac{p+|q|}{2}-k\right)!\left(\frac{p-|q|}{2}-k\right)!} r^{p-2k} \qquad (3)$$

where $0 \le |q| \le p$ and $p - |q|$ is even.

If N is the number of pixels along each axis of the image, then the discrete approximation of equation (1) is given as:

$$Z_{pq} = \lambda(p,N) \sum_{i=0}^{N-1} \sum_{j=0}^{N-1} R_{pq}(r_{ij}) e^{-\hat{j}q\theta_{ij}} f(i,j) \; ; 0 \le r_{ij} \le 1 \qquad (4)$$

where $\lambda(p,N)$ is normalizing constant and image coordinate transformation to the interior of the unit circle is given by

$$r_{ij} = \sqrt{x_i^2 + y_j^2} \; ; \theta = \tan^{-1}\left(\frac{y_j}{x_i}\right); \; x_i = c_1 i + c_2 \; ;$$

$$y_j = c_1 j + c_2 \qquad (5)$$

Since it is easier to work with real functions, Z_{pq} is often split into its real and imaginary parts, Z^c_{pq} , Z^s_{pq} as given below:

$$Z^c_{pq} = \frac{2(p+1)}{\pi} \int_0^{2\pi} \int_0^1 R_{pq}(r) \cos(q\theta) f(r,\theta) r dr d\theta \qquad (6)$$

$$Z^s_{pq} = \frac{2(p+1)}{\pi} \int_0^{2\pi} \int_0^1 R_{pq}(r) \sin(q\theta) f(r,\theta) r dr d\theta \qquad (7)$$

where $p \ge 0$, $q > 0$.

For the implementation, square image (N x N) is transformed and normalized over a unit circle; i.e. $x^2 + y^2 \le 1$, which the transformed unit circle image is bounding the square image. Figure 3 shows the square-to-circular transformation. In this transformation,

$$\lambda(p,N) = \frac{4(p+1)}{(N-1)^2 \Pi} \; ; \; c_1 = \frac{\sqrt{2}}{N-1} \; ; \; c_2 = \frac{-1}{\sqrt{2}} \qquad (6)$$

Therefore,

$$x_i = \frac{\sqrt{2}}{N-1} i + \frac{-1}{\sqrt{2}} \quad \text{and} \quad y_j = \frac{\sqrt{2}}{N-1} j + \frac{-1}{\sqrt{2}} \qquad (7)$$

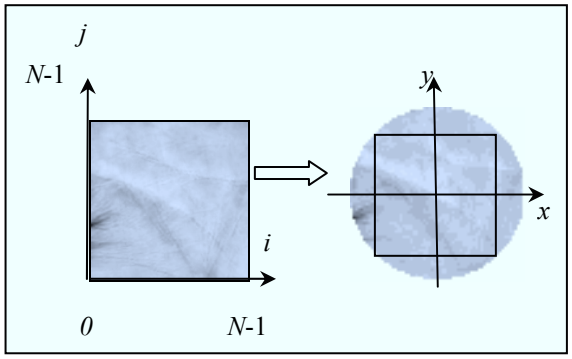

Figure 3. The square-to-circular transformation.

3.2. Pseudo Zernike Moments

The kernel of pseudo Zernike moments is the set of orthogonal pseudo Zernike polynomials defined over the polar coordinates inside a unit circle. The two-dimensional pseudo Zernike moments of order p with repetition q of an image intensity function $f(r,\theta)$ are defined as [Muk98a]:

$$PZ_{pq} = \frac{p+1}{\pi} \int_0^{2\pi} \int_0^1 PV_{pq}(r,\theta) f(r,\theta) r dr d\theta \qquad (8)$$

where Zernike polynomials $PV_{pq}(r,\theta)$ are defined as:

$$PV_{pq}(r,\theta) = PR_{pq}(r) e^{-\hat{j}q\theta} \; ; \quad \hat{j} = \sqrt{-1} \qquad (9)$$

and

$$r = \sqrt{x^2 + y^2} \; , \; \theta = \tan^{-1}\left(\frac{y}{x}\right), \; -1 < x, y < 1$$

The real-valued radial polynomials is defined as:

$$PR_{pq}(r) = \sum_{s=0}^{p-|q|} (-1)^s \frac{(2p+1-s)!}{s!(p+|q|+1-s)!(p-|q|-s)!} r^{p-s} \qquad (10)$$

and $0 \le |q| \le p, \; p \ge 0$

Since it is easier to work with real functions, PZ_{pq} is often split into its real and imaginary parts, PZ^c_{pq} , PZ^s_{pq} as given below:

$$PZ^c_{pq} = \frac{2(p+1)}{\pi} \int_0^{2\pi} \int_0^1 PR_{pq}(r) \cos(q\theta) f(r,\theta) r dr d\theta \qquad (11)$$

$$PZ^{s}_{pq} = \frac{2(p+1)}{\pi} \int_{0}^{2\pi} \int_{0}^{1} PR_{pq}(r) \sin(q\theta) f(r,\theta) r dr d\theta \quad (12)$$

where $p \geq 0$, $q > 0$.

Since the set of pseudo Zernike orthogonal polynomials is analogous to that of Zernike polynomial, most of the previous discussion for the Zernike moments can be adapted to the case of PZM.

We can see that the Zernike moments in equation (1) become pseudo Zernike moments if the radial polynomials, R_{pq}, defined as in equation (3) with its condition p-|q|=even is eliminated [Teh88a]. Therefore, pseudo Zernike moments offer more feature vectors than Zernike moments since pseudo Zernike polynomial contains $(p+1)^2$ linearly independent polynomials of order $\leq p$, whereas Zernike polynomial contains only $\frac{1}{2}(p+1)(p+2)$ linearly independent polynomials due to condition of p-$|q|$=even.

3.3. Legendre Moments

The kernel of Legendre moments is products of Legendre polynomials defined along rectangular image coordinate axes inside a unit circle. The (p,q) order Legendre moments are defined as:

$$\lambda_{pq} = \frac{(2p+1)(2q+1)}{4} \int_{-\infty}^{\infty} \int_{-\infty}^{\infty} P_p(x) P_q(y) f(x,y) dx dy \quad (13)$$

where the function $P_p(x)$ denote Legendre polynomial of order p. The Legendre moment generalizes the geometric moments in the sense that the monomial $x^p y^q$ is replaced by the orthogonal polynomial $P_p(x)$ $P_q(y)$ of the same order.

The discrete version of the Legendre moments can be written as

$$\lambda_{pq} = \frac{(2p+1)(2q+1)}{(M-1)(N-1)} \sum_{x=0}^{M-1} \sum_{y=0}^{N-1} p_p(x) p_q(y) f(x,y) \quad (14)$$

where (p+q) is the order, p,q=0,1,2,3,…, ∞.

The Legendre polynomials, $P_p(x)$ are a complete orthogonal basis set on the interval [-1,1]:

$$\int_{-1}^{1} p_p(x) p_q(y) dx = \frac{2}{2p+1} \delta_{pq} \quad (15)$$

the n^{th}–order Legendre polynomial are defined by

$$p_q(x) = \frac{1}{2^q} \sum_{p=0}^{\frac{q}{2}} (-1)^q \frac{(2q-2p)!}{p!(q-p)!(q-2p)!} x^{q-2p} \quad (16)$$

3.4. Moment reconstruction

By using moments, the palmprint image can be reconstructed from the extracted features. This vindicates the usefulness of moment to preserve the complete information in the extracted features. Figure 4 depicted palmprint image with its reconstructed images.

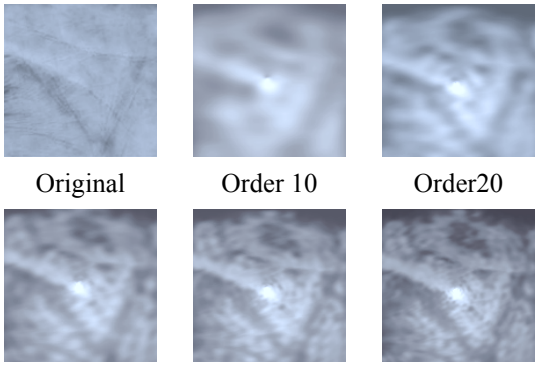

Figure 4. Original and reconstructed with different order palmprint images.

4. PALMPRINT VERIFICATION BASED ON ORTHOGONAL MOMENT'S FEATURES

A palmprint verification system is a one-to-one matching process. It matches a person's claimed identity to enrolled pattern. There are two phases in the system: enrollment and verification. Both phases comprise two sub-modules: preprocessing for palmprint localization, enhancement and feature extraction for moment features extraction. However, verification phase consists of an additional sub-module, classification, for calculating dissimilarity matching of the palmprint. Figure 5 shows the palmprint verification system block diagram.

At the enrollment stage, a set of the template images represented by moment features is labeled and stored into a database. At the verification stage, an input image is converted into a set of moment features, and then is matched with the claimant's palmprint image, based on the ID, stored in the database to gain the dissimilarity measure by computing Euclidean distance metric. We used this distance metric instead of more complex classification algorithm (e.g. neural network) because we were just focusing on the feature extracting rather than the classification. Finally, the dissimilarity measure is compared to a predefined threshold to determine whether a claimant should be accepted. If the dissimilarity measure below the predefined threshold value, the palmprint input is verified possessing same identity as the

claimed identity template and the claimant is accepted.

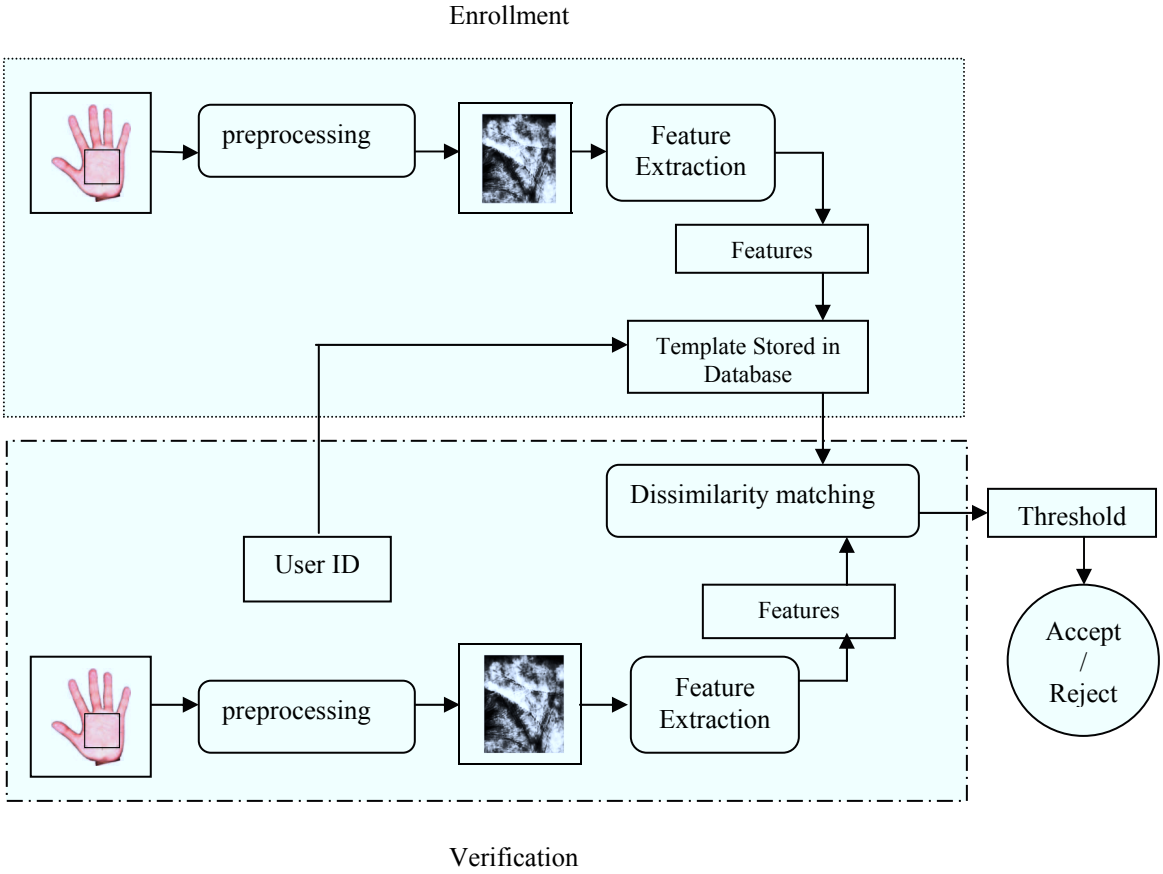

Figure 5. Block diagram of palmprint verification system.

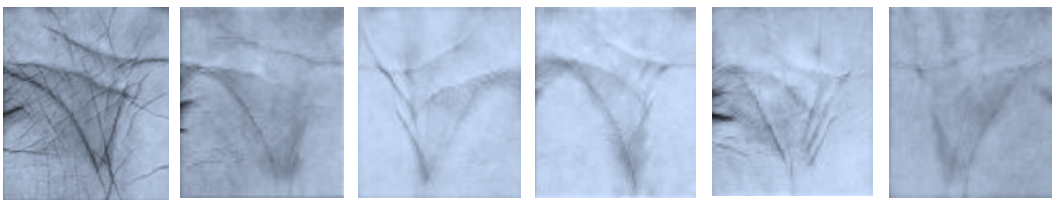

Figure 6. A few palmprint samples that used in the experiments.

5. EXPERIMENTAL STUDIES AND DISCUSSIONS

Experiments were conducted by using a set of database consisting of 50 different palmprint classes, with six samples for each class. This database is used to determine pertinent and optimal order moments in feature extraction before proceeding to next experimental study for computing FAR and FRR. Computation of FAR and FRR is to evaluate the overall performance of this authentication system. A few palmprint samples are shown in Figure 6.

At the first stage, database was used and experiment was conducted using different settings of feature vectors based on the order (h) of ZM, PZM and LM and the measure of class separability calculated by Euclidean distance is shown in Table 1.

Table 1 shows that setting 8 possesses the best feature vectors among the three orthogonal moments which can optimally describe the palmprint.

Furthermore, it also can be observed that the higher order moments extraction, the higher separability rate of the system as the higher order moments will capture finer details about the image. We also can observe that there is a large increment (approximately 40%) of the class separability rate between moments order 1 and order 3. However, feature extraction between higher order moments (e.g. between order 5 and order 7) just generated relatively small separability rate increment. This implies that informative and dominant characteristics of palmprint are placed in lower order moments but higher order moments impart flavor or nuance.

Note: $\Omega_h = \{Z_{pq}, PZ_{pq}, \lambda_{pq}\}$ where h is order

Feature Vectors		Measure of Class Separability (%)		
Settings	Feature Vector Elements	PZM	ZM	LM
1	Ω_0, Ω_1	52.0	36.0	36.0
2	$\Omega_0, \Omega_1, \Omega_2, \Omega_3$	91.3	78.7	88.0
3	$\Omega_0, \Omega_1, \Omega_2, \Omega_3, \Omega_4, \Omega_5$	95.3	90.7	96.7
4	$\Omega_0, \Omega_1, \Omega_2, \Omega_3, \Omega_4, \Omega_5, \Omega_6, \Omega_7$	96.0	96.0	97.3
5	$\Omega_0, \Omega_1, \Omega_2, \Omega_3, \Omega_4, \Omega_5, \Omega_6, \Omega_7, \Omega_8, \Omega_9$	97.3	96.0	98.0
6	$\Omega_0, \Omega_1, \Omega_2, \Omega_3, \Omega_4, \Omega_5, \Omega_6, \Omega_7, \Omega_8, \Omega_9, \Omega_{10}, \Omega_{11}$	98.0	96.7	98.0
7	$\Omega_0, \Omega_1, \Omega_2, \Omega_3, \Omega_4, \Omega_5, \Omega_6, \Omega_7, \Omega_8, \Omega_9, \Omega_{10}, \Omega_{11}, \Omega_{12}, \Omega_{13}$	98.0	96.7	98.7
8	$\Omega_0, \Omega_1, \Omega_2, \Omega_3, \Omega_4, \Omega_5, \Omega_6, \Omega_7, \Omega_8, \Omega_9, \Omega_{10}, \Omega_{11}, \Omega_{12}, \Omega_{13}, \Omega_{14}, \Omega_{15}$	98.0	98.0	98.7

Table 1. Recognition rate of ZM, PZM and LM using Euclidean distance

For the verification performance evaluation, a False Acceptance Rate (FAR) and a False Rejection Rate (FRR) test were performed. These measurements are defined as below:

$$FAR = \frac{number\ of\ accepted\ \ imposter\ claims}{total\ number\ of\ imposter\ accesses} \times 100\%$$

(17)

$$FRR = \frac{number\ \ of\ \ rejected\ \ client\ \ claims}{total\ \ number\ \ of\ \ client\ \ accesses} \times 100\%$$

(18)

These two measurements yield another performance measure, namely Total Success Rate (TSR):

$$TSR = \left(1 - \frac{FAR + FRR}{total\ number\ \ of\ accesses}\right) \times 100\%$$

(19)

The system performance can be evaluated by using Equal Error Rate (EER) where FAR=FRR.

A threshold value is obtained based on Equal Error Rate criteria where FAR=FRR. Threshold value of 0.4954, 0.3934 and 0.5314 is gained for PZM, PZM and LM respectively, as measure of dissimilarity. Figure 7 depicts an example experiment using Euclidean distance metric that determine threshold value based on EER criteria for PZM.

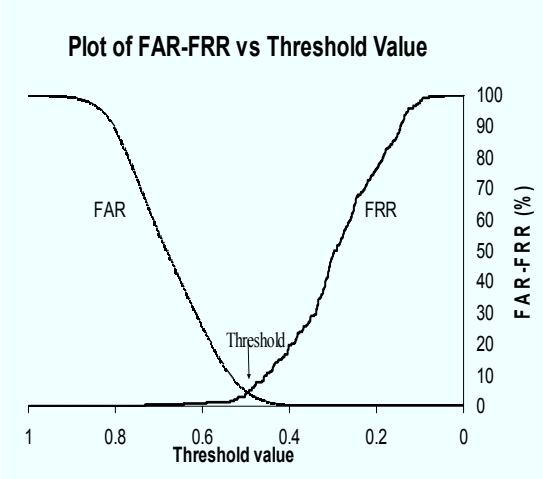

Figure 7. Plotted FAR-FRR graph to obtain threshold value for PZM.

Table 2 shows the testing result of verification rate with order moments from setting 8 (moments order 15) for ZM, PZM and LM, based on their defined threshold value.

moments	thres.	FAR(%)	FRR(%)	TSR(%)
PZM	0.4954	4.2449	4.4674	95.75
ZM	0.3934	5.2245	5.1546	94.78
LM	0.5314	4.5170	4.4674	95.48

Table 2. Testing result of verification rate of ZM, PZM and LM

The result demonstrates that application of using pseudo Zernike moments as feature extractor shows

the best verification performance among other moments. Figure 8 depicted plot of Receiver Operating Curve (ROC) of the three moments. From the figure, we can observe that pseudo Zernike moments shows its robustness in verification task since its curve is the lowest and the further left on the ROC graph.

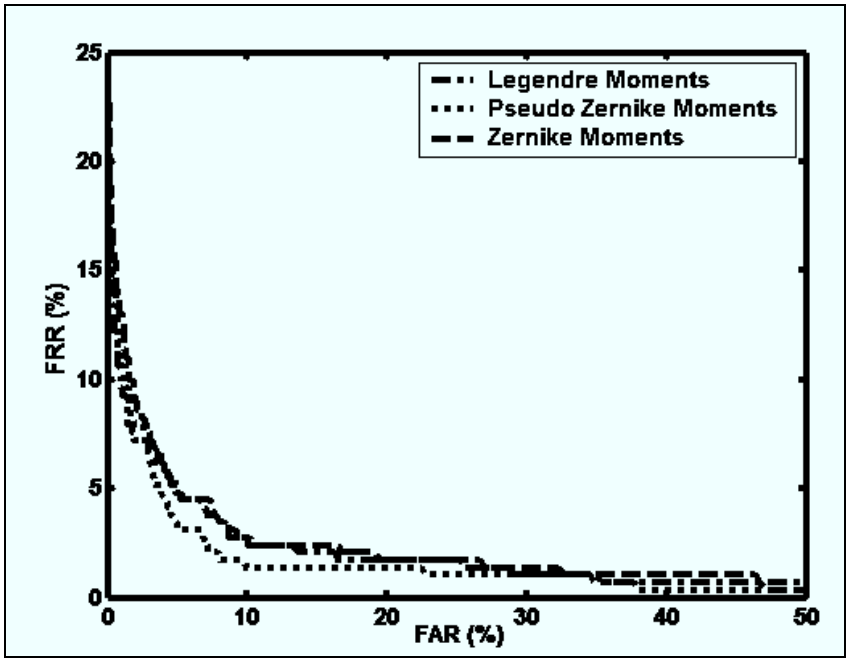

Figure 8. Plot of Receiver Operating Curve.

6. CONCLUSION

The performance of orthogonal moments: Zernike moments, pseudo Zernike moments and Legendre moments in the positive palmprint authentication system was presented in this paper. Higher orders of orthogonal moment contain more information about palmprint image and this improves the recognition rate. The pseudo Zernike moments of order 15 has the best performance among all the moments. Its verification rate is 95.75% with FAR = 4.2449% and FRR = 4.4674%, which represents the overall performance of this palmprint authentication system. The proposed algorithms, orthogonal moments, possess some advantages: orthogonality and geometrical invariance. Thus, they are able to minimize information redundancy as well as increase the discrimination power. Higher accuracy can be obtained by using more complex classifiers such as neural network.

7. ACKNOWLEDGEMENTS

Our thanks to Ms. Tee Connie for providing us the palmprint database. Besides, our highest appreciation also to Dr. Chong Chee Way for his information about moments.

8. REFERENCES

[Dav99a] David. Z., and Shu. W.. Two novel characteristics in palmprint verification: datum point invariance and line feature matching. Pattern Recognition, 32, pp. 691-702, 1999.

[Dut02a] Duta. N., Jain. A.K., and Mardia, K.V.. Matching of palmprint. Pattern Recognition Letters, 23, pp. 477-485, 2002.

[Hu62a] Hu. M.K,. Visual pattern recognition by moment invariant. IRE Trans. On Information Theory, vol. 8, No. 1, pp. 179-187, 1962.

[Kum02a] Kumar. A., and Shen H.C.. Recognition of palmprints using wavelet-based features. Proc. Intl. Conf. Sys., Cybern., SCI-2002, 2002.

[Li02a] Li. W., David. Z., and Xu. Z.. Palmprint identification by Fourier transform. Int. J. Patt. Recognition. Art. Intell., 16(4), pp. 417-432, 2002.

[Lu03a] Lu. G., David. Z., and Wang. K.. Palmprint recognition using eigenpalms features. Pattern Recognition Letters, 24(9-10), pp. 1473-1477, 2003.

[Muk98a] R. Mukundan and K.R. Ramakrishnan, Moment functions in image analysis – theory and applications. World Scientific Publishing, 1998.

[Shu98a] Shu Wei and D. Zhang. Palmprint verification: an implementation of biometric technology. Proceedings of ICRP'98, Brisbane, Queensland, Australia, pp. 219-221, Aug. 1998.

[Tee02a] Tee Connie, Michael Goh, Andrew Teoh, and David Ngo. An automated biometric palmprint verification system. 3rd Int. Symp. On Communications & Info. Tech. (ISCIT2003), vol. 2, pp. 714-719, 2002.

[Teh88a] C.H. Teh and R.T. Chin. On image analysis by the methods of moments. IEEE Trans. Pattern Anal. Machine Intell., vol. 10, pp. 496-512, July 1988.

[Wai03a] Wai. K.K., David. Z., and Li. W.. Palmprint feature extraction using 2-D Gabor filters. Pattern Recognition, 36(10), pp. 2339-2347, 2003.

[Wu02a] X. Wu, K. Wang and D. Zhang. Fuzzy Directional Element Energy Feature (FDEEF) based palmprint identification. Internet Conf. Pattern Recognition, vol. 1, Quebec City, Canada, Aug. 2002.

[You02a] J. You, W. Li and D. Zhang. Hierarchical palmprint identification via multiple feature extraction. Pattern Recognition, vol. 35, pp. 847-859, 2002.